Studies of Stability and Reactivity of Synthetic Cryptomelane-like Manganese Oxide Octahedral Molecular Sieves

Yuan-Gen Yin,[†] Wen-Qing Xu,[†] Roberto DeGuzman,[†] and Steven L. Suib*[,†,‡,§]

Department of Chemistry, Department of Chemical Engineering, and Institute of Materials Science, University of Connecticut, Storrs, Connecticut 06269-3060

C. L. O'Young*

Texaco Research Center, Texaco, Inc., P.O. Box 509, Beacon, New York 12508

Received April 6, 1994[⊗]

Cryptomelane is known to be a manganese oxide octahedral molecular sieve having a well-defined 2 × 2 tunnel structure (OMS-2) with K^+ situated in tunnel positions. The mobility and reactivity of oxygen in such tunnel structures with different tunnel cations were studied by means of temperature-programmed desorption (TPD) and reduction with H_2 and CO_2. Oxygen released during TPD from OMS-2 materials is significantly greater in amount than that from OMS-1 (3 × 3 tunnel structure), although the relative populations of oxygen from different desorption temperature regimes are much the same as that of OMS-1. Oxygen species corresponding to low-temperature, medium-temperature, and high-temperature TPD peaks can be assigned to weakly bound chemisorbed dioxygen, oxygen atoms bound to lower valent Mn ions, and those bound to Mn^{4+} ions in the framework, just as is the case for OMS-1. Among the different tunnel cations, Cu^{2+} exhibits a distinct feature of having more available oxygen species that are reactive at low temperature. The availability of oxygen in Cu^{2+}-doped OMS-2 was also studied by frontal reduction at 563 K with CO/He. The amount of oxygen depleted during frontal reduction is close to that during TPR by CO/He. The depleted Cu^{2+} hollandite can be reoxidized to about 85% recovery of oxygen by oxygen pulse reactions. X-ray diffraction patterns show that the 2 × 2 tunnel structure remains intact after heating in an oxygen-free gas stream up to 778 K, but collapses after reduction in CO at 563 K. These studies emphasize the importance of pretreatment of OMS materials prior to use in catalysis or adsorption.

I. Introduction

Manganese oxides possess highly diverse crystallographic morphologies. A family of layered and tunnel structures is possible with MnO_6 octahedra as the structural unit. Among the tunnel structures, todorokite is the most attractive owing to its vast presence in the tremendous resource of deep-sea nodules. For industrial applications as adsorbents or catalysts, synthetic todorokite is more appropriate while extreme diversification in composition and structure occurs for the mineral todorokite in various deep-sea nodules.[1] Previous studies have revealed some interesting catalytic behavior[2] and the presence of several different oxygen species[3] in doped todorokites, having a 3 × 3 tunnel structure with a pore opening of 6.9 Å. This material is known as OMS-1, and its composition and structure are given in Figure 1.

The α-MnO_2 phase has a well-defined 2 × 2 tunnel structure, and is composed of double chains of edge-shared MnO_6 octahedra and corner-sharing of the double chains. Its smaller opening (4.6 Å in size) probably imparts higher stability to its structure. Related minerals are cryptomelane (with K^+ as tunnel cation) and hollandite (with Ba^{2+} as tunnel cation). In this laboratory, α-MnO_2 complexes with different doping cations, such as Cu^{2+}, Ni^{2+}, Co^{2+}, and K^+, were synthesized and showed interesting electrochemical behavior.[4] These octahedral molecular sieves (OMS) have been studied here in order to understand more about lability of oxygen species in such systems. These α-MnO_2 materials are designated generically as OMS-2, as differentiated from OMS-1 which has the todorokite 3 × 3 tunnel structure. The structure and composition of OMS-1 are given in Figure 1.

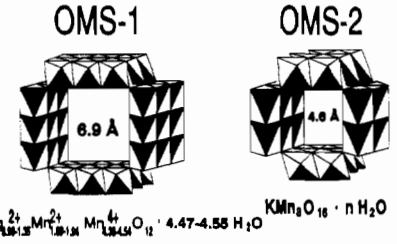

Figure 1. Structures and compositions of octahedral molecular sieves: (A) synthetic todorokite, OMS-1; (B) synthetic cryptomelane, OMS-2.

In view of the smaller tunnel size of OMS-2 and possible closer proximity of tunnel cation positions to the framework oxygens and manganese ions, the presence and behavior of oxygen species in OMS-2 materials have been investigated here by means of temperature-programmed techniques. We have compared oxygen species in OMS-2 to those in OMS-1 in two aspects in this research. On one hand, the peak positions in the temperature-programmed desorption (TPD) or temperature-

* To whom correspondence should be addressed.
† Department of Chemistry, University of Connecticut.
‡ Department of Chemical Engineering, University of Connecticut.
§ Institute of Materials Science, University of Connecticut.
⊗ Abstract published in *Advance ACS Abstracts,* August 15, 1994.

(1) Chukhrov, F. V.; Gorshov, A. I.; Dritz, V. A. *Izv. Akad. Nauk. SSSR, Ser. Geol.* **1985**, 61.
(2) Shen, Y. F.; Zerger, R. P.; Suib, S. L. *Science* **1993**, *260*, 511.
(3) Yin, Y. G.; Xu, W. Q.; Shen, Y. F.; Suib, S. L.; O'Young, C. L. *Chem. Mater.*, in press.
(4) DeGuzman, R.; Shen, Y. F.; Neth, E. J.; Suib, S. L.; O'Young, C. L.; Levine, S.; Newsam, J. M. *Chem. Mater.*, in press.

0020-1669/94/1333-4384$04.50/0

programmed reduction (TPR) data are measures of stability or reactivity of oxygen species. On the other hand, the area under the peak is a measure of the availability of oxygen species in specific temperature regimes. In addition, the redox behavior of Cu hollandite was further investigated by frontal reduction with CO/He and pulse oxidation with oxygen. These data may be useful in redox catalysis and other applications of OMS materials.

II. Experimental Section

A. Synthesis. OMS-2 materials doped with Cu, Ni, K, and Fe were synthesized by refluxing a mixture of potassium permanganate, manganous sulfate, and corresponding metal nitrates in aqueous solution for 24 h.[4] Their X-ray diffraction patterns are in accord with literature data for cryptomelane.

B. Temperature Program Techniques. Temperature-programmed desorption (TPD) in an inert atmosphere and temperature-programmed reduction (TPR) with hydrogen or carbon monoxide of OMS-2 materials were carried out as described in the literature.[3] Cu—OMS-2 was subjected to frontal reduction by carbon monoxide at 563 K. A Pyrex reactor of 4 mm internal diameter was loaded with 10 mg of Cu—OMS-2, over which a stream of 4.90% CO in He at a steady flow rate of 6.8 sccm was introduced to replace He. The effluent was passed through a thermal conductivity detector (TCD) after a liquid nitrogen (LN_2) trap to condense carbon dioxide that was formed. After the CO/He stream showed a steady TCD signal, the Pyrex tube containing Cu—OMS-2 was placed into a tubular furnace maintained at 563 K to start the reduction. There was a brief dip in reduction temperature of 7−8 K within 20 s which recovered to the specified temperature after 90 s.

The consumption of CO in He was monitored by the TCD signal and the flow of CO/He was stopped when the TCD signal reached the base line, showing that reduction by CO is complete at this temperature. Cu—OMS-2 materials were reoxidized after this frontal reduction by introducing oxygen pulses, separated by an interval of 3 min, at the same temperature, with a short period of He purging to remove CO. The consumption of oxygen in each pulse was monitored via the change in thermal conductivity of remaining oxygen in the He stream after condensing the water formed with an ethanol/LN_2 trap. The consumption of both carbon monoxide and oxygen was calibrated by means of TPR of freshly calcined CuO of the same weight or by measuring oxygen in a loop of known volume.

C. X-Ray Diffraction. The X-ray powder diffraction patterns of Cu—OMS-2 after various treatments were collected by using a Scintag 2000 XDS diffractometer with Cu Kα X-ray radiation. A 0.02 step in 2θ/count, a beam voltage of 45 kV, and a beam current of 40 mA were used.

III. Results

A. TPD and XRD Experiments. Figure 2 shows the TPD spectra of OMS-2 doped with different cations. Apparently, these spectra mainly show a predominant high-temperature (HT) peak generally above 850 K in addition to some low-temperature (LT) and medium-temperature (MT) peaks of much lower intensity. The MT peaks are not well resolved, especially because their tails are merged with the front of the HT peaks. The envelopes as a whole are similar to the TPD spectra of doped OMS-1[3] and manganese dioxide,[5] as well as manganite perovskites.[6,7] There are no particular temperature cutoffs or protocol for the LT, MT, and HT regimes.

X-ray diffraction patterns for Cu—OMS-2 samples subjected to TPD to 563, 778, and 943 K are shown in Figure 3, together with data for untreated Cu—OMS-2. Similar diffraction lines are observed for the untreated and treated materials up to and including 778 K.

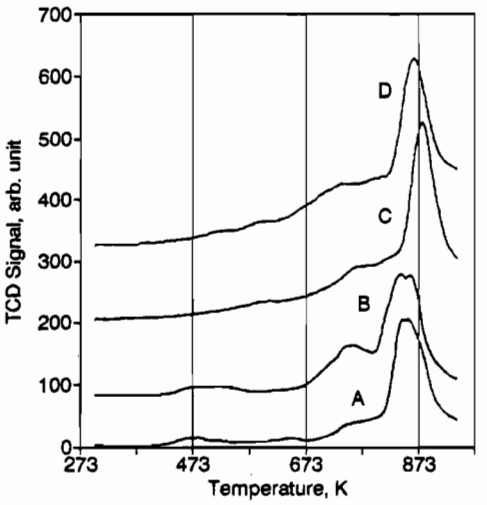

Figure 2. TPD spectra of OMS-2 with different tunnel cations in He: (A) K^+—OMS-2; (B) Cu^{2+}—OMS-2; (C) Fe^{3+}—OMS-2; (D) Ni^{2+}—OMS-2.

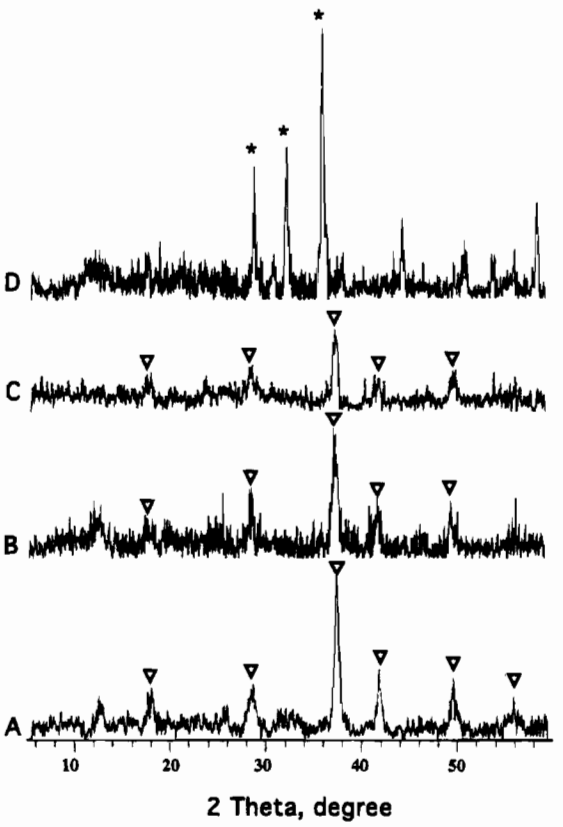

Figure 3. X-ray diffraction patterns of Cu—OMS-2 after TPD to different temperatures: (A) untreated sample; (B) sample after TPD to 563 K; (C) sample after TPD to 778 K; (D) sample after TPD to 943 K. Key: (∇) OMS-2; (*) Mn_2O_3.

B. TPR Experiments. The TPR H_2/Ar spectra, as shown in Figure 4, are characterized by a predominant sharp MT peak together with some minor LT peaks. These H_2/TPR spectra appear to be unlike the H_2/TPR spectra of doped OMS-1.[3] However, they bear more resemblance to TPD spectra of corresponding doped OMS-2 materials, although they emerge at much lower temperature. Another dissimilarity to the H_2/Ar TPR spectra of OMS-1 is the significantly smaller influence exerted by the doping cation.

(5) Iwamoto, M.; Yoda, Y.; Yamazoe, N.; Seiyama, T. *J. Phys. Chem.* **1978**, *82*, 2564.
(6) Seiyama, T.; Yamazoe, N.; Eguchi, K. *Ind. Eng. Chem., Prod. Res. Dev.* **1985**, *24*, 19.
(7) Petunchi, J. O; Lombardo, E. A. *Catal. Today* **1990**, *8*, 201.

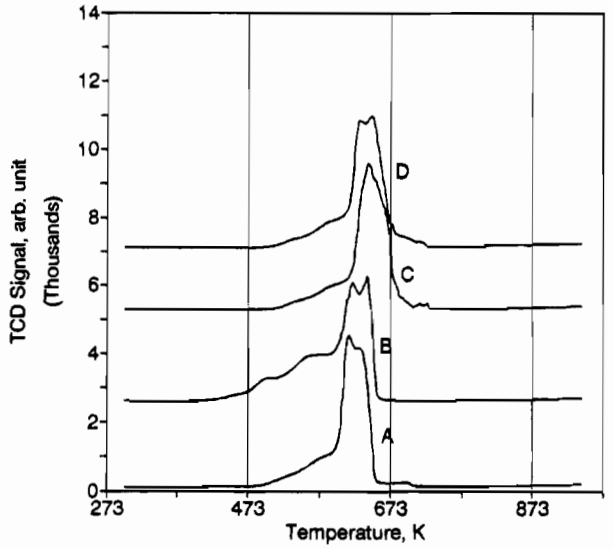

Figure 4. TPR spectra of OMS-2 with different tunnel cations in H_2/Ar: (A) Fe^{3+}—OMS-2; (B) Ni^{2+}—OMS-2; (C) K^+—OMS-2; (D) Cu^{2+}—OMS-2.

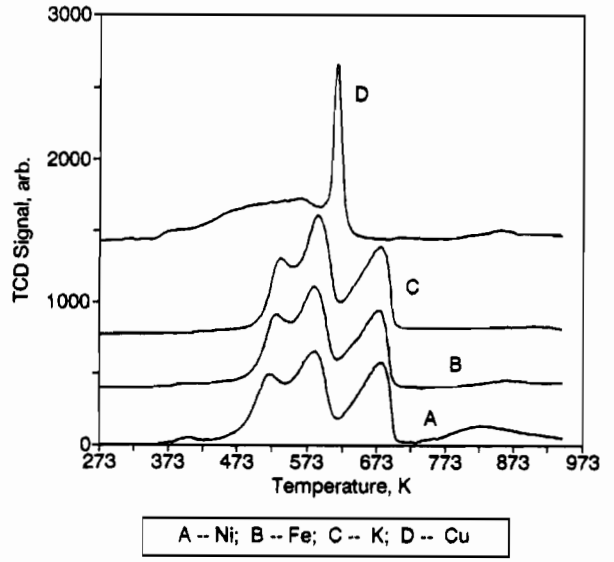

Figure 5. TPR spectra of OMS-2 with different tunnel cations in CO/He: (A) Ni^{2+}—OMS-2; (B) Fe^{3+}—OMS-2; (C) K^+—OMS-2; (D) Cu^{2+}—OMS-2.

The CO/TPR spectra are shown in Figure 5. The OMS-2 samples containing Ni, Fe, and K in tunnel sites manifest quite similar behavior to the CO/He TPR data in the moderate- (MoT) to medium-temperature (MT) regimes, with Ni—OMS-2 showing small TPR peaks in the LT and HT regimes. However, Cu—OMS-2 behaves in quite a different manner. There are a multitude of low-intensity LT peaks, adjoining each other and forming a continuous broad band, followed by a spike in the medium—high-temperature (MHT) region for Cu—OMS-2 as shown in Figure 5d.

C. Frontal Reductions. Figure 6 shows the result of frontal reduction of Cu—OMS-2 by CO/He at 563 K. The CO consumed amounts to 1.60 μmol/mg. Subsequently, 22 oxygen pulses were passed at 563 K. Figure 7 shows the change in TCD signal with pulse number, revealing significant uptake of oxygen by the depleted Cu—OMS-2 materials. An X-ray diffraction pattern for the Cu—OMS-2 material after frontal reduction by CO/He and subsequent oxygen pulses is shown in Figure 8.

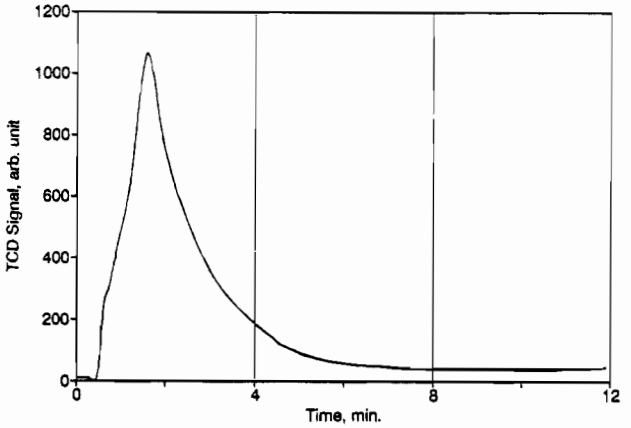

Figure 6. Frontal reduction of Cu—OMS-2 by CO/He at 563 K.

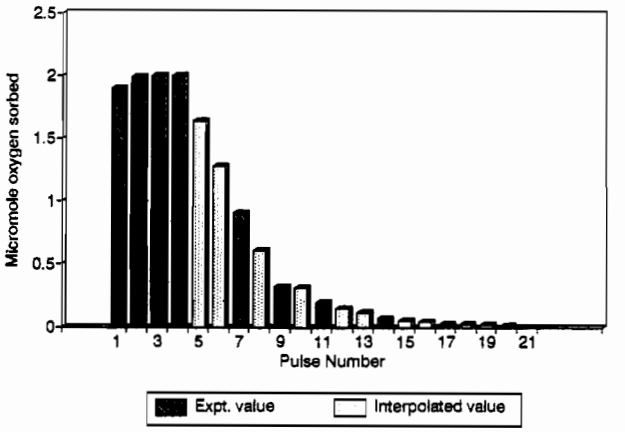

Figure 7. Removal of oxygen in 22 oxygen pulses passed through Cu—OMS-2 after reduction by CO/He at 563 K.

V. Discussion

A. Structural Considerations. There have been several studies of crystal structures of natural and synthetic hollandites.[8-11] Modeling of these structural data has suggested that K^+ and Rb^+ ions are in tunnel positions. The X-ray diffraction pattern of K—OMS-2 synthesized in our laboratory without using hydrothermal treatment[4] has also been subjected to Rietveld refinement. It was shown that modeling with K^+ ions presumed to be in tunnel positions leads to a good match with the X-ray diffraction data, thus fortifying the suggestion that K^+ ions occupy tunnel sites.[4] Meanwhile, the similarity of X-ray diffraction patterns of OMS-2 samples doped with Ni, Fe, and Cu to that of K—OMS-2 lends inference that doped cations in these OMS-2 samples synthesized in our laboratory also occupy tunnel sites of the 4.6 Å tunnels of OMS-2 shown in Figure 1. Hereafter, these cations are referred to as tunnel cations.

B. The Nature and Amounts of Desorbed Oxygen Species. The TPD spectra of OMS-2 samples of Cu, Ni, Fe, and K shown in Figure 2 all have features similar to those of MnO_2, manganite perovskites, and doped OMS-1, i.e., a predominant peak in the high-temperature regime which is only slightly changed by substitution of different cations in tunnel sites. This point has been discussed in a previous paper for transition metal OMS-1 materials.[3] In the case of OMS-2 materials, structural investigation on both natural[8-10] and synthetic[11] samples showed that the bond distance between tunnel cations and oxygen is

(8) Post, J. E.; Von Dreele, R. B.; Buseck, P. R. *Acta Crystallogr.* **1982**, *B38*, 1056.
(9) Post, J. E.; Burnham, C. W. *Am. Mineral.* **1986**, *71*, 1178.
(10) Miura, H. *Mineral. J.* **1986**, *13*, 119.
(11) Yamamoto, N.; Oka, Y.; Tamada, O. *Mineral. J.* **1990**, *15*, 41.

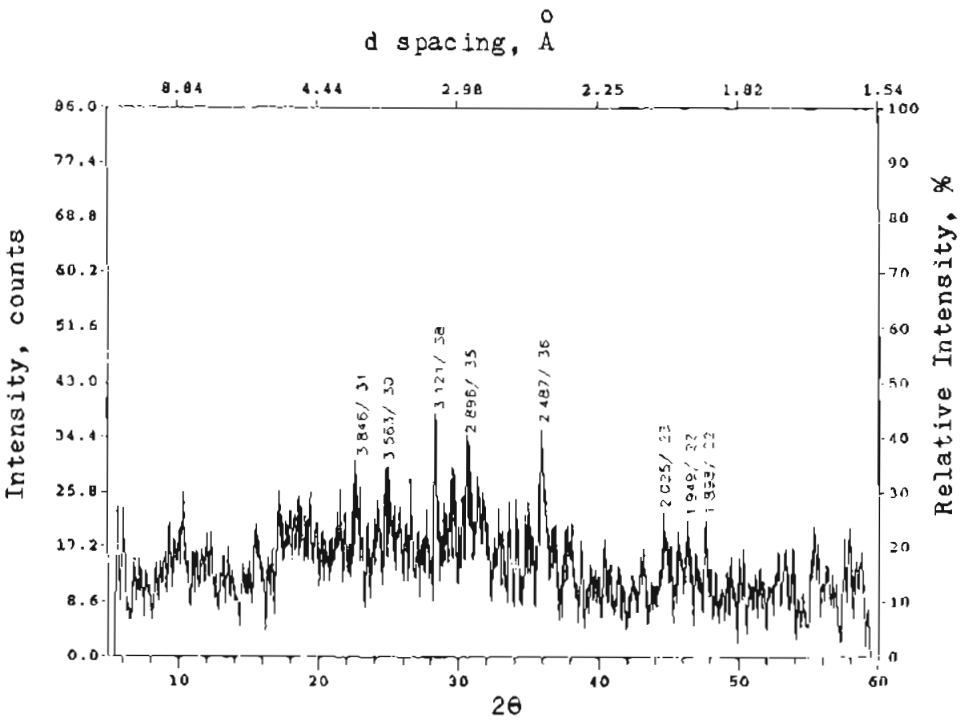

Figure 8. X-ray diffraction pattern of Cu—OMS-2 after reduction—reoxidation treatment.

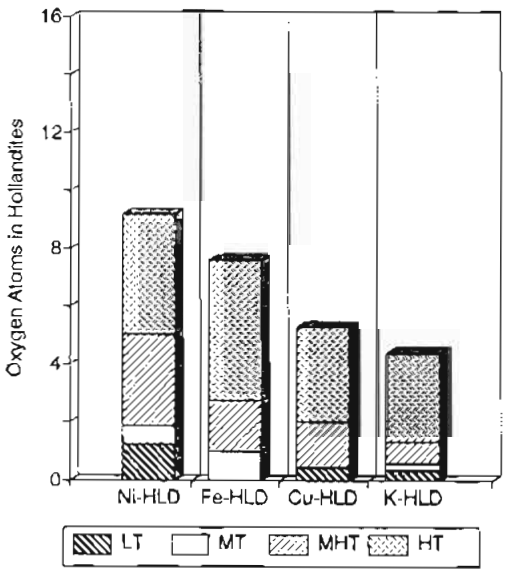

Figure 9. Distribution of oxygen species in TPD of OMS-2.

generally 2.89 Å. Although the tunnel cation may be closer to the oxygen ions in OMS-2 as compared to OMS-1, which has a larger tunnel, such cations may still be too far apart to have a considerable influence on the mobility of oxygen species in comparison to the expected major influence of manganese ions in framework position. In addition, the transition metal dopants are present at a level of <5 wt % in all cases, whereas the total Mn content is more like 50—60 wt %.

The doped OMS-2 samples are assigned a formula $TMn_8O_{16}\cdot H_2O$, in which T = Cu^{2+}, Ni^{2+}, Fe^{3+}, and K^-. After the amount of oxygen released from OMS-2 is calculated by comparing the peak area in the TPD to that of oxygen pulses from a loop of known volume, a distribution of oxygen species corresponding to LT, MT and HT peaks can be derived as shown in Figure 9. The assignment of oxygen species desorbed in these temperature regimes discussed in a previous paper[3] still seems valid for the case of OMS-2. For example, at low temperatures, adsorbed molecular oxygen is evolved, in an intermediate regime, adsorbed atoms are desorbed, and at high temperatures, lattice oxygen is released.

It is observed that the total amount of oxygen released from doped OMS-2 samples (during TPD) ranges from 4.4 (in K—OMS-2) to 9.2 (in Ni—OMS-2)) oxygen atoms per molecule, and is much greater than those from doped OMS-1 materials. From the thermogravimetric analysis (TGA) results of DeGuzman et al.,[3] the loss of oxygen in K—OMS-2 when heated to 948 K in a nitrogen atmosphere can be estimated to be about 2.6 atoms per molecule. Keeping in mind that the weight loss in TGA experiments changes significantly around 948 K for M—OMS-2 samples, the estimate of total O desorbed from TPD data agrees more or less with the TGA result.

HT peaks in M—OMS-2 samples (see Figure 2) are 40—70 K higher than those in OMS-1, in accord with the expectation that OMS-2 should possess higher thermal stability due to its more compact tunnel structure. Comparison of the thermal stability via TPD is consistent with TGA results for OMS-1[2] and OMS-2.[4] However, more oxygen is evolved in the medium- to high-temperature regimes during TPD from OMS-2 than OMS-1. This can be rationalized by the difference in oxygen content of the decomposition products of OMS-1 and OMS-2. For example, OMS-2 is known to decompose above 873 K to Mn_2O_3,[4] which would have a lower oxygen content than the decomposition product of OMS-1, if the latter is presumed to be thermally decomposed to a spinel TMn_2O_4 structure and Mn_2O_3.[2]

As the LT peaks in TPD spectra are rather low in intensity (making quantitation difficult), and the HT peak intensities do not differ much for various OMS-2 samples, significant differences in the intensities of peaks in the MT and MHT regime (573—783 K) reveal a minor influence of tunnel cation. The positions of the HT peaks shift to lower temperature in the order $Fe^{3+} > Ni^{2+} > K^+ > Cu^{2+}$. Excluding the monovalent alkaline cation K^+, this order of decreasing thermal stability parallels the order of decreasing ionic radius. Similar trends were also

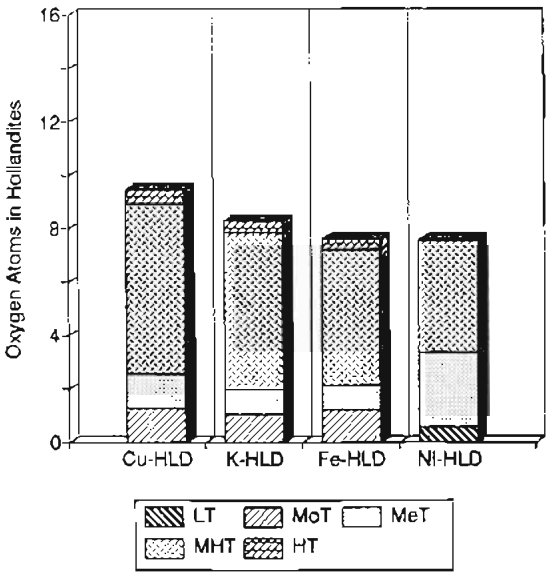

Figure 10. Distribution of oxygen species in TPR of OMS-2 in H_2/Ar.

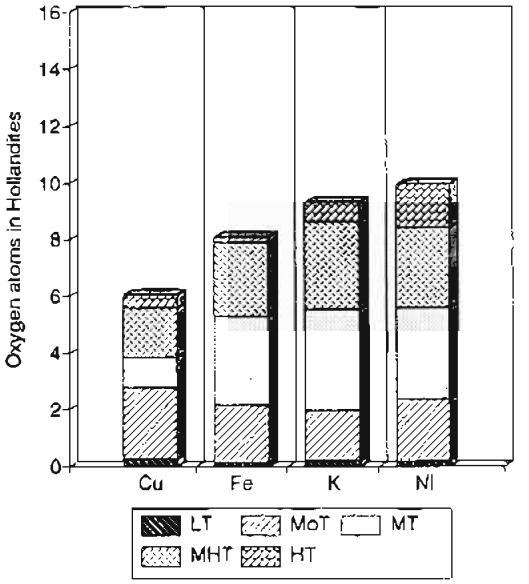

Figure 11. Distribution of oxygen species in TPR of OMS-2 in CO/He.

observed between the stability of $AMnO_3$ perovskites and the ionic radii of A cations.[12]

The X-ray diffraction patterns shown in Figure 3 demonstrate that Cu—OMS-2 is essentially stable up to 778 K even in an oxygen-free gas stream. Cu—OMS-2 seems to retain its tunnel structure effectively, even after losing about 2 atoms of oxygen per molecule during TPD to 778 K; cf. Figure 9. However, heating to 943 K in an oxygen-free gas stream culminates in a phase change of the sample. The resulting compound is well-crystallized and can be identified by XRD as Mn_2O_3(T). These data support our belief that OMS-2 has excellent thermal stability.

B. Reduction of OMS-2 Materials with Hydrogen OMS-2 Materials. The reduction of metal hollandites seems to be more facile than lanthanum manganite perovskites on the basis of comparison of H_2 TPR data. For the latter, it was reported[7] that the minimum temperature required for complete reduction is 1015 K. Fierro et al.[13] observed an initial reduction temperature for the TPR of lanthanum manganite perovskite to be 755 K. Vogel et al.[14] reported an even higher temperature of 1323 K for the reduction of Mn^{3+} to Mn^{2+} in the TPR of $LaMnO_3$.

Exhaustive reduction of OMS-2 at such a high temperature (>1000 K) would result in collapse of the tunnel structure of OMS-2. Evidently, the OMS-2 samples are much more susceptible to reduction, as a reduction of Mn^{4+} to lower valency is involved; meanwhile reduction of Mn^{3+} to Mn^{2+} is involved for TPR of manganite perovskite systems. The relative ease with which oxygen species can be released from OMS-2 implies higher oxidation activity, as has been shown in the case of manganite perovskite.[15]

From the TPR/H_2 spectra of various metal containing OMS-2 materials (Figure 4), the population of oxygen species reactive to hydrogen corresponding to TPR peaks emerging in different temperature regimes can be calculated after calibration with the same weight of freshly calcined CuO. These results are shown in Figure 10. These data suggest that about 56−71% of the OMS-2 oxygen available for reduction is concentrated in a narrow temperature range of 590−670 K (MHT species) and 24−37% is available in a temperature regime of 535−595 K (MoT and MT species). Less than 10% of the OMS-2 oxygen reactive to H_2 is found as either a LT peak for Ni—OMS-2 (460 K) or as an HT peak for other M—OMS-2 samples (>690 K).

Such highly uneven populations are in distinct contrast to the much broader population in OMS-1 (except Cu—OMS-1) for which the reactive oxygen for H_2 reduction spans a range of 523−800 K. Another feature of OMS-2 reduction by H_2 distinct from OMS-1 (as can be seen from Figure 10) is the less pronounced effect of doping cation. The total amount of oxygen available for H_2 reduction ranges from 7.7 to 9.5 atoms for OMS-2 doped with different cations; that for OMS-1 ranges from 8.1 to 13.1. Again, the OMS-2 materials show higher stability to H_2 reduction than OMS-1.

C. Reduction of OMS-2 Samples with CO. As for the TPR/CO data of Figure 5, the three main peaks for K—, Fe—, and Ni—OMS-2 materials are readily discerned, allowing calculation of distributions of oxygen species in a rather straightforward manner, as shown in Figure 11. However, the TPR spectra of Cu—OMS-2 of Figure 5d is rather difficult to be resolved; integration with a Hewlett-Packard GC integrator resulted in an overall area under a broad band. We had to deconvolute this broad peak with the SigmaPlot program, assuming a 4-component Lorentzian peak shape with 12 parameters. As the space for constraints to be imposed on the parameters are not sufficient, the best fit we obtained is shown in Figure 12. In principle, it would better to deconvolute into five components in order to achieve a better fitting. Due to, first, limitations imposed by the program, and, second, our opinion that the analysis does not warrant a more sophisticated resolution, the demarcation of oxygen species in Cu—OMS-2 seems satisfactory. The population of oxygen species reactive to CO is also shown in Figure 11.

The tunnel cation seems to exert a more pronounced influence on oxygen availability in OMS-2 to CO oxidation when compared to that for H_2 oxidation. Again, excluding the monovalent K^+ ion, the oxygen availability decreases in the order $Ni^{2+} > Fe^{3+} > Cu^{2+}$, paralleling the order of decreasing ionic radius, as with TPD results. However, the influence of Ni^{2+} and Cu^{2+} in OMS-2 on the oxygen availability for CO oxidation is significantly less in the case of OMS-2, as compared to the case of OMS-1.[3] Among the tunnel cations, the influence

(12) Tejuca, L. G.; Fierro, J. L. G. *Adv. Catal.* **1989**, *26*, 260.
(13) Fierro, J. L. G.; Tascòn, J.; Tejuca, L. G. *J. Catal.* **1984**, *89*, 209.
(14) Vogel, E. M.; Johnson, D. W., Jr.; Gallagher, P. K. *J. Am. Ceram. Soc.* **1977**, *60*, 31.
(15) Libby, W. F. *Science* **1971**, *171*, 499.

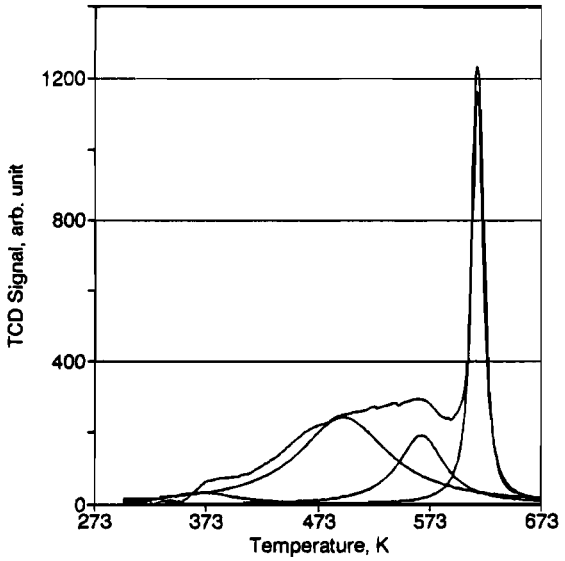

Figure 12. Deconvolution of TPR/CO spectrum of Cu—OMS-2.

exerted by Cu^{2+} is particularly noteworthy, with respect to both the lowest peak temperatures and the least amount of oxygen available during TPR/CO. Note again that Cu—OMS-2 possesses also the largest amount of oxygen available in TPR/H_2 experiments (i.e., Figure 4).

D. Frontal Reduction of Cu—OMS-2. The amount of oxygen atoms in Cu—OMS-2 depleted in frontal reduction with CO/He at 563 K (see Figure 6) was calculated, by calibrating with the same weight of freshly calcined CuO, to be 2.5. Meanwhile, the oxygen atoms removed from Cu—OMS-2 during TPR/CO (Figure 5) up to 563 K is calculated to be 3.0, essentially in fair agreement with the result from frontal reduction if the initial unsteady period of about 1 min is taken into consideration.

The initial brief dip of about 3—7 K in reduction temperature lasts just $^1/_3$ min. There could be an initial short induction period even after the stabilization of reduction temperature. After that induction period, the reduction of Cu—OMS-2 by CO/He proceeds in a single stage, as can be seen from the reduction curve (Figure 6). However, as the TCD signal does not return to the base line, the depletion of the pertinent oxygen species does not terminate but proceeds at a very slow rate. Such phenomena seem to be due to the overlapping of oxygen species in this temperature regime, as evidenced from the TPR/CO envelope of Cu—OMS-2 (Figure 5d).

After frontal reduction, the depleted Cu—OMS-2 was treated with 22 successive oxygen pulses at the same temperature in order to encourage reoxidation as shown in Figure 7. The amount of oxygen atoms reincorporated into the depleted Cu—OMS-2 during pulse reaction is calculated to be 2.1, i.e., a recovery of 85%. Generally speaking, for a catalytic oxidation reaction to proceed smoothly according to the Mars—van Krevelen redox mechanism, the rate of reoxidation of depleted catalyst usually significantly exceeds the rate of reduction of catalyst. Although in-depth kinetic studies of these redox reactions are not yet available, the above result may cast some doubts of the compatibility of reoxidation rates with reduction rates for Cu—OMS-2.

X-ray diffraction patterns for Cu—OMS-2 after frontal reduction with CO/He and reoxidation, Figure 8, shows a poorly crystallized compound. This demonstrates that the tunnel structure of Cu—OMS-2 can not be restored after reduction—reoxidation treatments used in this study. However, as the OMS-2 materials are synthesized by either reflux or calcination methods, there exists the possibility of restoration of the 2 × 2 tunnel structure by heating different materials in an oxygen atmosphere under appropriate conditions. Comparison of XRD patterns in Figure 8 to trace D of Figure 3 suggests the possible presence of finely dispersed Mn_2O_3(T). Obviously, heating to higher temperature with removal of oxygen in the absence of reductant leads to well-crystallized products that might be important electronic, magnetic and battery materials.

VI. Conclusions

The following conclusions were reached in our TP studies reported here.

(1) TPD spectra and related oxygen species distributions of OMS-2 bear resemblance to those of OMS-1. Tunnel size does not significantly affect the relative ratio of oxygen species released in different temperature regimes into an oxygen-free gas stream.

(2) Smaller tunnel size plays a minor role in determining stability of oxygen in OMS-2 against TPD and TPR in H_2. The oxygen in OMS-2 reactive to H_2 is highly concentrated in a narrow temperature range as compared to OMS-1 materials.

(3) While the amount of oxygen released during TPD is significantly larger from OMS-2 than from OMS-1, the amounts of oxygen reactive to H_2 or CO in OMS-2 are considerably smaller than those in OMS-1 systems.

(4) Tunnel cations affect the distribution of oxygen species either during TPD or TPR. Cu—OMS-2 is unique among the OMS-2 samples studied here as regards abundant reactive oxygen species at low temperatures. Cu—OMS-2 materials are also quite stable and retain their tunnel structure even after heating in an oxygen-free gas stream up to 573 K with loss of 1/8 of their total oxygen atoms (per unit cell).

(5) A great majority of oxygen can be recovered by Cu—OMS-2 after a mild reduction of Cu—OMS-2 (563 K) in CO. However, the tunnel structure can not be restored after reoxidation.

Acknowledgment. We acknowledge Texaco, Inc., and the Office of Basic Energy Sciences, Division of Chemical Sciences, Department of Energy, for support of this research.